Acta Biomaterialia 6 (2010) 1978–1991

Contents lists available at ScienceDirect

Acta Biomaterialia

journal homepage: www.elsevier.com/locate/actabiomat

Injectable, rapid gelling and highly flexible hydrogel composites as growth factor and cell carriers

Feng Wang [a], Zhenqing Li [a], Mahmood Khan [b], Kenichi Tamama [b], Periannan Kuppusamy [b], William R. Wagner [c], Chandan K. Sen [b], Jianjun Guan [a,*]

[a] Department of Materials Science and Engineering, The Ohio State University, Columbus, OH 43210, USA
[b] Davis Heart and Lung Research Institute, The Ohio State University, Columbus, OH 43210, USA
[c] McGowan Institute for Regenerative Medicine, Departments of Surgery, Chemical Engineering and Bioengineering, University of Pittsburgh, Pittsburgh, PA 15219, USA

ARTICLE INFO

Article history:
Received 26 September 2009
Received in revised form 1 December 2009
Accepted 4 December 2009
Available online 23 December 2009

Keywords:
Hydrogel
Composite
Release
Human mesenchymal stromal cell
Insulin-like growth factor

ABSTRACT

A family of injectable, rapid gelling and highly flexible hydrogel composites capable of releasing insulin-like growth factor (IGF-1) and delivering mesenchymal stromal cell (MSC) were developed. Hydrogel composites were fabricated from Type I collagen, chondroitin sulfate (CS) and a thermosensitive and degradable hydrogel copolymer based on *N*-isopropylacrylamide, acrylic acid, *N*-acryloxysuccinimide and a macromer poly(trimethylene carbonate)-hydroxyethyl methacrylate. The hydrogel copolymer was gellable at body temperature before degradation and soluble at body temperature after degradation. Hydrogel composites exhibited LCSTs around room temperature. They could easily be injected through a 26-gauge needle at 4 °C, and were capable of gelling within 6 s at 37 °C to form highly flexible gels with moduli matching those of the rat and human myocardium. The hydrogel composites showed good oxygen permeability; the oxygen pressure within the hydrogel composites was similar to that in the air. The effects of collagen and CS contents on LCST, gelation time, injectability, mechanical properties and degradation properties were investigated. IGF-1 was loaded into the hydrogel composites for enhanced cell survival/growth. The released IGF-1 remained bioactive during a 2-week release period. Small fraction of CS in the hydrogel composites significantly decreased IGF-1 release rate. The release kinetics appeared to be controlled mainly by hydrogel composite water content, degradation and interaction with IGF-1. Human MSC adhesion on the hydrogel composites was comparable to that on the tissue culture plate. MSCs were encapsulated in the hydrogel composites and were found to grow inside during a 7-day culture period. IGF-1 loading significantly accelerated MSC growth. RT-PCR analysis demonstrated that MSCs maintained their multipotent differentiation potential in hydrogel composites with and without IGF-1. These injectable and rapid gelling hydrogel composites demonstrated attractive properties for serving as growth factor and cell carriers for cardiovascular tissue engineering applications.

1. Introduction

Hydrogels are a class of biomaterials that have high water content and tissue-like mechanical properties [1,2]. Hydrogels alone or combined with cells have been used to engineer a variety of tissues in vitro and in vivo [3–5]. Injectable hydrogels as one hydrogel type have been extensively employed as cell carriers for in vivo tissue engineering [6,7]. The advantages of using injectable hydrogels lie in that they have high moldability, capable of filling irregular-shaped defects; can be delivered to the in vivo environment by limited surgical invasion such as minimally invasive surgery [8]; and are readily for cell and drug encapsulation. After being delivered in vivo, the injectable hydrogels solidify to form tissue constructs, which are exposed to the in vivo environment and therefore are capable of experiencing local biological and mechanical cues that may enhance tissue development [9,10].

Injectable hydrogel solidification (gelation) can be accomplished by approaches including chemical polymerization, photopolymerization and thermal crosslinking [6,11–13]. The chemical polymerization and photopolymerization have been extensively applied for gelation of injectable hydrogels, though the use of chemicals (initiators) in the processes may raise cytotoxicity issues or add complexity to the delivery systems [12]. Thermal crosslinking is applicable for thermosensitive hydrogels that undergo phase separation in response to temperature change [14]. The gelation can be achieved simply by raising the temperature to above lower critical solution temperature (LCST) of the polymer. Various thermosensitive hydrogels such as methylcellulose [15], poly(*N*-isopropylacrylamide) (PNIPAAm) and copolymers [14,16],

* Corresponding author. Tel.: +1 614 292 9743.
E-mail address: guan.21@osu.edu (J. Guan).

1742-7061/$ - see front matter © 2009 Acta Materialia Inc. Published by Elsevier Ltd. All rights reserved.
doi:10.1016/j.actbio.2009.12.011

poly(ethylene oxide)–poly(propylene oxide)–poly(ethylene oxide) (PEO–PPO–PEO) [6,14,16], poly(ethylene glycol) (PEG)/biodegradable polyester copolymers [6,14,16,17], and elastin-like peptides [18] have been developed. Poly(*N*-isopropylacrylamide) (PNIPAAm) is one of the most studied thermosensitive polymers due to its relatively low LCST (32 °C), allowing it to be in the gel form at body temperature. PNIPAAm has been utilized for a broad range of applications such as drug delivery [19] and cell therapy [20,21]. The major limitation for PNIPAAm hydrogel is that it is non-biodegradable and not readily cleared away from the body under physiological conditions [22]. Efforts have been made to prepare degradable PNIPAAm by introduction of biomacromolecules or peptide sequences into the PNIPAAm-based polymers [23], or copolymerization with monomers possessing degradable polyester segments [11–12]. Another disadvantage limiting the application of PNIPPAm hydrogel is its intrinsic hard and brittle mechanical properties. To address these two limitations, we have previously developed a family of biodegradable and flexible PNIPAAm based hydrogels using PLA as a degradable segment [11]. Although these hydrogels exhibited attractive mechanical properties, they are not yet ideal as they have relatively high degradation rates and low cytocompatibility.

Our objective in this work was to synthesize a slower degrading PNIPAAm based hydrogel that also possess attractive mechanical properties, and develop a family of composites capable of improving cytocompatibility and delivery bioactive factors and cells. To accomplish these objectives, a thermosensitive copolymer based on *N*-isopropylacrylamide, acrylic acid, *N*-acryloxysuccinimide and a macromer poly(trimethylene carbonate)-hydroxyethyl methacrylate (HEMAPTMC) was synthesized. The hydrogel was found to have significantly reduced degradation rate than previous hydrogels using PLA as a degradable segment [11]. Collagen and chondroitin sulfate were incorporated in the hydrogel and developed a family of hydrogel composites with improved cytocompatibility. Furthermore, prosurvival growth factor IGF-1 was loaded into the hydrogel composites. The IGF-1 loading significantly enhanced MSC growth within the hydrogel composites. The chemical, mechanical and degradation properties of the resulting hydrogel and hydrogel composites, IGF-1 release kinetics, cell adhesion and growth were evaluated.

2. Materials and methods

2.1. Materials

Trimethylene carbonate (TMC, Boehringer Ingelheim) was lyophilized overnight to remove residual water prior to use. NIPAAm (Acros) was recrystallized in ethyl acetate and hexane, respectively. Acrylic acid (AAc, Fisher Scientific) and 2-hydroxyethyl methacrylate (HEMA, Sigma) were purified by reduced pressure distillation. *N*-Acryloxysuccinimide (NAS, Sigma), benzoyl peroxide (BPO, Fisher Scientific), stannous 2-ethylhexanoate ($Sn(OCt)_2$, Fisher Scientific), Type I acid soluble collagen (Kensey Nash Corporation) and chondroitin sulfate A sodium salt (CS, Sigma) were used as received. Solvents used in the experiments were analytical grade.

2.2. Synthesis of polytrimethylcarbonate-hydroxyethyl methacrylate (HEMAPTMC) macromer

Macromer HEMAPTMC was synthesized by ring-opening polymerization of TMC with HEMA (Scheme 1) [11,24]. The reaction was carried out under N_2 atmosphere. TMC and HEMA with a molar ratio of TMC/HEMA = 2 were added into a three-necked flask equipped with N_2 inlet and outlet. The flask was placed in an 110 °C oil bath. After TMC was melted, $Sn(OCt)_2$ (1 mol.% with respect to HEMA) dissolved in 1 ml toluene was added. The reaction was conducted at 110 °C for 1 h. The flask was then cooled to room temperature, and added with tetrahydrofuran (THF) to dissolve the reaction mixture. The solution was precipitated in ice water. The precipitate was dissolved in ethyl acetate and dried with $MgSO_4$ overnight. After filtration, the ethyl acetate was evaporated under reduced pressure. The resulting viscous oil was then dried in a vacuum oven overnight at room temperature. The synthesized macromer was characterized by ^1H NMR using chloroform ($CDCl_3$) as a solvent. The HEMA/TMC ratio in the macromer was 1.9 as calculated from area of the protons from HEMA unit (CH_2 = 6.02 and 5.68 ppm, respectively; CH_3– 1.95 ppm; –OCH_2CH_2O– 4.33 ppm) and TMC unit (–O$CH_2CH_2CH_2$O– 4.11 ppm; –O$CH_2CH_2CH_2$O– 1.91 ppm).

2.3. Synthesis of hydrogel copolymer poly(NIPAAm-co-AAc-co-NAS-co-HEMAPTMC)

Poly(NIPAAm-co-AAc-co-NAS-co-HEMAPTMC) was synthesized by free radical polymerization using benzyl peroxide (BPO) as an initiator (Scheme 1) [11]. Monomers NIPAAm, AAc, NAS and HEMAPTMC with a molar ratio of 85/6/5/4 were dissolved in 1,4-dioxane to form a 10 wt.% monomer solution and added into a 500 ml one-necked flask. The flask was purged with N_2 for 10 min. A degassed solution of BPO (7.2×10^{-3} mol/mol monomer) in 1,4-dioxane was then injected into the flask. The polymerization was conducted at 70 °C for 24 h. After cooling to room temperature, the polymer solution was precipitated in hexane. The polymer was purified twice by dissolving in THF and precipitating in ethyl ether. The resulting polymer was dried at 50 °C in a vacuum oven.

2.4. Preparation of hydrogel/collagen and hydrogel/collagen/chondroitin sulfate composites

The hydrogel/collagen composites were prepared by mixing hydrogel with Type I collagen (Scheme 2). This process involved conjugation reaction between NHS groups in the hydrogel and amine groups in the collagen [11]. The hydrogel copolymer was dissolved in phosphate buffered saline (PBS, pH 7.4) at 4 °C to form a 20 wt.% solution. The defined amount of Type I collagen solution (8 wt.%) was neutralized with small aliquots of 1 M sodium hydroxide, and then added into the hydrogel solution. After thoroughly mixing, the hydrogel/collagen mixture was set at 4 °C overnight. The collagen content initially added to the hydrogel solution was 5 and 10 wt.%, respectively. To prepare hydrogel/collagen/CS composite, CS was added to above collagen incorporated hydrogel mixture. The CS/collagen ratio of 6 wt.% was used [25,26]. The formed composites were placed in a 37 °C water bath for gelation to obtain gels. The poly(NIPAAm-co-AAc-co-NAS-co-HEMAPTMC) copolymer hydrogel, hydrogel/collagen and hydrogel/collagen/CS composites were abbreviated as Tgel, Tgel/ColX and Tgel/ColX/CS, respectively, where Col, CS and X represent collagen, chondroitin sulfate A sodium salt and collagen content, respectively. Three different kinds of hydrogel composites were made by varying collagen content and addition of CS (Table 1).

2.5. Polymer characterization

Polymer molecular weight was measured by gel permeation chromatography (GPC, Waters 1515 HPLC pump, Waters 2414 differential refractometer) at 35 °C using THF as a solvent. Poly(methyl methacrylate) standards (Fluka, ReadyCal Set M_p 500–2,700,000) were used for calibration. ^1H NMR spectra were recorded by a 300 MHz spectrometer employing $CDCl_3$ as a solvent. Glass transition temperatures (T_gs) of the dry polymer composites

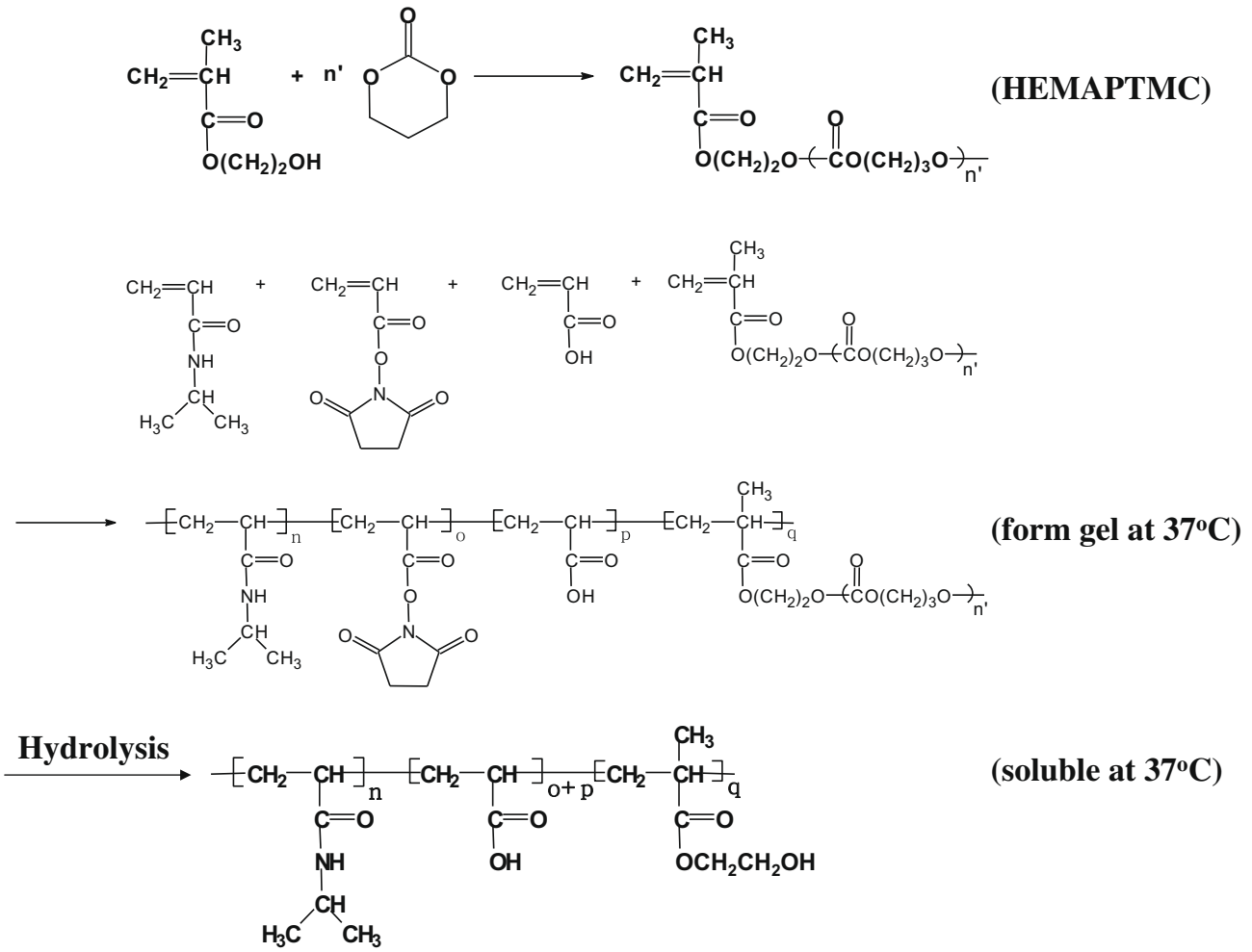

Scheme 1. Synthesis of macromer HEMAPTMC and copolymer poly(NIPAAm-*co*-AAc-*co*-NAS-*co*-HEMAPTMC), and degradation of the copolymer.

were measured by differential scanning calorimetry (DSC, TA 2920) over a temperature range of −100 to 200 °C using a heating rate of 20 °C min^{-1}. Dry polymer composites were prepared by lyophilization of hydrogel composite solutions. LCSTs of the hydrogel composites were determined by DSC over a temperature range of 0–90 °C using a heating rate of 10 °C min^{-1}. The hydrogel composite solutions containing 20 wt.% hydrogel copolymer were used for all studies. LCST of the completely degraded hydrogel was also measured. The completely degraded hydrogel was prepared by hydrolysis of hydrogel copolymer in a 1.0 M sodium hydroxide solution at 4 °C for 10 days, followed by neutralization with a 10 M hydrochloride solution. Complete degradation was judged by the observation of a clear hydrogel solution when placed in a 37 °C water bath since its LCST was above 37 °C (Table 2). Molecular weight of the completely degraded polymer was also measured.

Hydrogel composite gelation time was measured in a microscope (IX71, Olympus) equipped with a temperature control system (Weather Station, Precisioncontrol, Inc.) and a video recorder (DP70, Olympus). The system was pre-warmed to 37 °C before testing. During the testing, a drop of hydrogel composite solution (20 μl, 20 wt.%) pre-cooled to 4 °C was quickly dropped on the glass slide placed on the stage of the microscope. The gelation process was recorded. The time needed for the hydrogel solution to become completely opaque (light is completely blocked) was considered as a gelation time. Hydrogel composite injectability was evaluated by its ability to be injected through a 26-gauge needle. This was based on the consideration for future animal injection, where needles as small as 26-gauge were used. Hydrogel composite solution (4 °C) was filled into a 1 ml syringe equipped with a 26-gauge needle. The syringe was then cooled in a 4 °C refrigerator before being manually injected.

Water content of the hydrogel composites at 37 °C was measured. The hydrogel composite solutions containing 20 wt.% of hydrogel copolymer were placed in a 37 °C water bath for gelation. The formed gels were maintained at 37 °C for 5 h to reach equilibrium water content. The gels were then taken out and wiped with tissue paper to remove the surface water. Water content was defined as the difference between the wet mass (w_2) and dry mass (w_1) of the hydrogel composites:

$$\text{Water content } (\%) = 100 \times (w_2 - w_1)/w_1$$

Oxygen permeability of the hydrogel composites was tested using electron paramagnetic resonance (EPR) oximetry. The principle of EPR oximetry is based on molecular oxygen-induced linewidth changes in the EPR spectrum of a paramagnetic probe. EPR technology has been well established and validated for measurements of oxygen pressure P_{O_2} from single cell to whole organ [27–29]. EPR oximetry was conducted using established procedure as described previously [27]. A stable and non-toxic paramagnetic LiNc-BuO was used as a probe. The probe was sonicated to less than 1 μm in size and mixed with hydrogel before loaded in gas-permeable capillary tube for EPR measurements. The gas-perme-

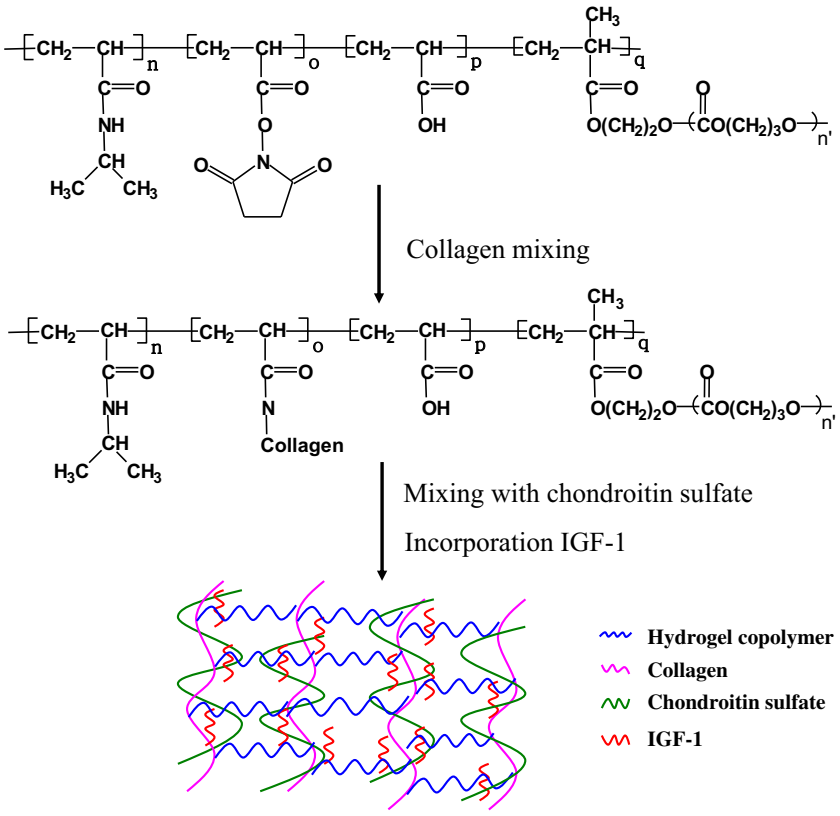

Scheme 2. Fabrication of hydrogel composites. The fabrication process includes mixing of hydrogel with collagen, incorporation of chondroitin sulfate and IGF-1 loading.

Table 1
Composition of hydrogel and hydrogel composites.[a]

	Hydrogel (wt.%)	Collagen (wt.%)	CS (wt.%)
Tgel	100	0	0
Tgel/Col5	95	5	0
Tgel/Col10	90	10	0
Tgel/Col5/CS	95	5	0.3

[a] The hydrogel copolymer concentration was 20 wt.% for all the hydrogel and hydrogel composite solutions.

Table 2
Gelation time, injectability and water content of hydrogel composites.[a]

	Gelation time (s)[b]	Injectability[c]	Water content (wt.%)
Tgel	5	+	43 ± 2
Tgel/Col5	4	+	56 ± 5
Tgel/Col10	6	+	58 ± 3
Tgel/Col5/CS	5	+	50 ± 2
Tgel/Col5 + MSC	5	+	—
Tgel/Col5/CS + MSC	5	+	—

[a] The hydrogel copolymer concentration was 20 wt.% for all the hydrogel and hydrogel composite solutions.
[b] Gelation time was tested at 37 °C for 20 μl of hydrogel composite.
[c] Injectability was tested through a 26-gauge needle.

able tube was flushed with 100% N_2 for 17 min to remove any oxygen in the hydrogel composites. Similarly, it was flushed with 21% O_2 for 17 min to allow oxygen penetrate into the hydrogel composites. The P_{O_2} measurements were performed using an L-band EPR spectrometer (Magnettech, Berlin, Germany). EPR spectra were acquired as single 60 s duration scans. The instrument settings were: microwave frequency, 1.2 GHz (L-band); incident microwave power, 4 mW; modulation amplitude, 180 mG; modulation frequency 100 kHz; receiver time constant, 0.2 s. The peak-to-peak width of the EPR spectrum was used to calculate P_{O_2} using a standard calibration curve [27].

Tensile mechanical properties of the hydrogel composites at 37 °C were characterized using the method described previously [14]. Before testing, 2 ml of 20 wt.% hydrogel composite solution in a 20 ml vial were placed in a 37 °C water bath to form a gel. The gel was maintained in the water bath for 5 h before being removed from the vial and cut into a rectangular shape with a width of 3 mm and a length of 25 mm. To ensure that the sample loading process does not cause sample defects due to thermosensitive nature of the hydrogel composites, the grips were preheated at 37 °C before the samples being loaded. The testing was conducted in a 37 °C water bath using an Instron load frame (model 1322). A cross-head speed of 50 mm min^{-1} was used [30]. At least five samples were evaluated for each condition.

2.6. Hydrogel degradation

Hydrogel composites degradation in PBS (pH 7.4) at 37 °C was quantified for Tgel, Tgel/Col5 and Tgel/Col5/CS over a 2-week degradation period. The defined volume (~250 μl) of thoroughly mixed hydrogel composite solution with defined concentration (~20 wt.%) was added into a 2 ml microcentrifuge tube. The hydrogel composite solution was placed in a 37 °C water bath for gelation and the formed gel was maintained in the water bath for 5 h. The supernatant (water repelled during the gelation) was then taken out and pre-warmed PBS was added. The degradation was conducted at 37 °C. The samples were taken at defined intervals, washed three times with warm DI water and vacuum dried at 60 °C for 2 days before being weighed (w_2). The weight remaining was calculated as:

$$\text{Weight remain } (\%) = 100 \times w_2/w_1$$

where w_1 is the sample weight before degradation. At least four samples were evaluated for each hydrogel composite type.

2.7. Cytotoxicity of degradation products

The cytotoxicity of hydrogel copolymer degradation products was evaluated by their effect on NIH3T3 fibroblast growth [31]. The hydrogel copolymer was completely degraded using the method described in Section 2.5. Different amount of degradation products were dissolved in the normal culture medium (Dulbecco's modified Eagle's medium (DMEM) with 10% FBS) to obtain media containing different concentration of degradation products (1, 5, 10 and 15 mg ml^{-1}). The cells were seeded into a 96-well tissue culture plate at a density of 2×10^5 cells ml^{-1} and supplemented with normal culture medium. After 24 h of culture, the medium was removed and replaced with medium containing degradation products. The normal culture medium without degradation products was used a control. After 48 h of culture, cell viability was evaluated by MTT assay.

2.8. IGF-1 loading and release

IGF-1 was loaded into Tgel/Col5 and Tgel/Col5/CS to fabricate IGF-1 releasing hydrogel composites (Scheme 2). IGF-1 (PeproTech Inc.) was dissolved in PBS (pH 7.4) to obtain a stock solution with a concentration of 100 μg ml^{-1}. The defined volume (~8 μl) of IGF-1 solution was then added into 1 ml, 4 °C hydrogel composite solution containing 20 wt.% of hydrogel copolymer. The IGF-1 concentration was designed to be 40 ng mg^{-1} dry hydrogel composite. After thoroughly mixing, the mixture was kept at 4 °C overnight. The mixture was then transferred into a 37 °C water bath for gelation to obtain an IGF-1 encapsulated gel (~210 mg in dry weight). To measure release kinetics of the IGF-1, the gel was remained in the water bath for 5 h before the supernatant was collected and 2 ml release medium was added. The PBS supplemented with 1% penicillin/streptomycin and 0.5% fetal bovine serum (FBS) was used as a release medium [32,33]. The release was conducted in a 37 °C water bath. The release medium was collected at predetermined time intervals and replaced with fresh release medium. The concentration of IGF-1 in the release medium was measured by IGF-1 ELISA kit (R&D systems). The IGF-1 loading efficiency was defined as:

$$\text{Loading efficiency} = (w_1 - w_2)/w_1 \times 100\%$$

where w_1 and w_2 are amount of IGF-1 initially added into the hydrogel composite and amount of IGF-1 in the supernatant (water repelled during the gelation), respectively.

2.9. Bioactivity of released IGF-1

Bioactivity of released IGF-1 was evaluated in terms of its stimulatory effect on NIH3T3 fibroblast growth [34]. The cells were cultured in a T-175 flask supplemented with a culture medium containing 10% FBS and DMEM. The cells were seeded into a 96-well tissue culture plate at a density of 2×10^5 cells ml^{-1}. After incubation for 24 h, the culture medium was removed and replaced with above collected IGF-1 containing release medium. The cells were then cultured for additional 48 h and cell viability was measured by MTT assay [11]. The release media without IGF-1, with 1 and 10 ng ml^{-1} IGF-1 were used as controls.

2.10. MSC adhesion on hydrogel composites

Hydrogel composite surface was seeded with MSCs to evaluate cell adhesion. Human MSCs (Lonza) were expanded in T-175 flasks supplemented with undifferentiation culture medium (DMEM containing 20% FBS, 100 U ml^{-1} penicillin, 100 μg ml^{-1} streptomycin and 2 mM L-glutamine). The culture medium was changed twice a week. MSCs at passage 10 were used for cell seeding. Previous study demonstrated that MSCs at this passage preserved multipotency and phenotype [35]. Hydrogel and hydrogel composites were cut into 6 mm discs and fitted into a 96-well tissue culture plate. MSCs were seeded at a density of 2×10^5 cells ml^{-1} on the samples. After 24 h of culture, the culture medium was removed and the samples were washed with 37 °C PBS for three times. The cells and hydrogel composites were then digested with trypsin, neutralized with FBS and diluted with large amount of PBS (4 °C). The cell number was quickly counted using a hemocytometer. Before counting, both cell suspension and hemocytometer were cooled at 4 °C to allow the cell suspension to be transparent during the counting. MSC adhesion on pure hydrogel (Tgel), hydrogel composites (Tgel/Col5 and Tgel/Col5/CS) with or without IGF-1 loading was evaluated ($n = 5$). Tissue culture plate was used as a control.

2.11. MSC encapsulation in hydrogel composite

The hydrogel composites with or without IGF-1 loading were encapsulated with MSCs to evaluate the effect of IGF-1 loading on MSC growth within the hydrogel. MSCs at passage 10 were used. Before encapsulation, MSCs were labeled with living cell marker CellTracker Green CMFDA (5-chloromethylfluorescein diacetate, concentration 10 μM) at 37 °C for 30 min [11]. The labeled MSCs were washed twice with culture medium to remove free CMFDA. The MSCs were then suspended in PBS to obtain a cell suspension with a density of 1×10^7 cells ml^{-1}. The hydrogel composites (containing 20 wt.% of hydrogel copolymer) solutions with or without IGF-1 loading were sterilized under UV light in a laminar flow hood for 30 min at 4 °C. The labeled MSC suspension (0.25 ml) was mixed thoroughly with 1 ml of hydrogel composite solution obtain a final cell density of 2.5×10^6 cells ml^{-1}. The mixture was transferred into a 37 °C water bath for gelation for 10 min to obtain MSC encapsulated hydrogel composites. The supernatant was then removed and replaced with culture medium (PBS containing 20% FBS, 100 U ml^{-1} penicillin, 100 μg ml^{-1} streptomycin and 2 mM L-glutamine). Cell encapsulation efficiency was calculated as the percentage of number of cells encapsulated (number of cells added minus number of cells in the supernatant) to number of cells originally added. The medium was changed daily for 7 days. After 1, 3 and 7 days of culture, the hydrogel composites were digested with trypsin, neutralized with FBS and diluted with a large amount of PBS (4 °C). The cell number was counted using a hemocytometer as described above. To image live cells, the hydrogel composites were cut into ~100 μm thick pieces and visualized using a fluorescent microscope.

RT-PCR analysis was performed for MSCs encapsulated in the hydrogel composites after 7 days' culture. The MSCs cultured in tissue culture plate were used as control. Total RNA was extracted by TRIzol (Sigma) according to the manufacturer's instruction. Amount of isolated RNA was quantified by Nanodrop 1000 (Thermo, USA). Approximately 1 μg RNA was used to synthesize cDNA by High Capacity cDNA Reverse Transcription Kits (Applied Biosystem). PCR was performed by Mastercycler ep gradient S thermal cycler (Eppendorf) and Platinum *Taq* DNA Polymerase (Invitrogen) with primers listed in Table 3 by the conditions below: 94 °C for 2 min, 40 cycles (94 °C for 1 min, 58 °C for 1 min and 72 °C for 2 min) and a final 72 °C extension for 10 min [36]. The amplified product was analyzed by electrophoresis in 2% agarose gel.

Table 3
PCR primers.

Gene	Prime sequences (Forward and Reverse)	T_m (°C)[a]
Collagen Type 1 (α1)	5′-CCGGAAACAGACAAGCAACCCAAA-3′	73.2
	3′-AAAGGAGCAGAAAGGGCAGCATTG-5′	71.8
Osteonectin	5′-TTCTGCCTGGAGACAAGGTGCTAA-3′	69.8
	3′-TCTGTTACTTCCCTTTGCCCACCT-5′	69.4
PPARγ2	5′-CTGTTTGCCAAGCTGCTCCAGAAA-3′	72.1
	3′-AAGAAGGGAAATGTTGGCAGTGGC-5′	71.6
β-Actin	5′-AAGATCAAGATCATTGCTCCTC-3′	61.2
	3′-GGACTCATCGTACTCCTG-5′	59.5

[a] T_ms were calculated by NIH PerlPrimer software.

To evaluate mechanical properties after MSC encapsulation, the MSC encapsulated hydrogel composites were placed in a 37 °C water bath for 5 h to reach equilibrium water content. The mechanical properties of the formed gels were tested at 37 °C according to the method described above. At least five samples were tested for each condition.

2.12. Statistical methods

Data are expressed as mean value ± standard deviation. Statistical analysis was performed by ANOVA with post hoc Neuman–Keuls testing for differences.

3. Results

3.1. Characterization of hydrogel copolymer

FTIR and ^{1}H NMR spectra were used to characterize structure of the synthesized hydrogel copolymer. FTIR spectrum (Fig. 1a) shows that the copolymer had characteristic absorptions of amide group (1530 and 1640 cm^{-1}), isopropyl group (1460, 1380 and 1360 cm^{-1}), carboxylic group (1713 cm^{-1}), succinimide group (1780 and 1806 cm^{-1}) and carbonate group (1730 cm^{-1}), respectively. In ^{1}H NMR spectrum (Fig. 1b), the copolymer demonstrated characteristic proton peaks of the monomer units NIPAAm (a, b, c, d and e), AAc (a and b), NAS (a, b and f) and HEMAPTMC (a, g, h, i and j). Composition of the synthesized copolymer was calculated from the integration area ratio of the characteristic proton peaks from each monomer unit, NIPAAm (c), AAc (a/2-c-f/4-g/3), NAS (f/4) and HEMAPTMC (g/3). The NIPAAm/AAc/NAS/HEMAPTMC ratio was found to be 85.0/5.8/5.5/3.7. The number average molecular weight of the copolymer was 31,000 (PDI 1.72) as characterized by GPC.

3.2. Hydrogel composites gelation time, injectability, oxygen permeability and water content

Hydrogel composites were formed by mixing of hydrogel and collagen, with or without addition of CS. Collagen content affected hydrogel composite gelation ability. When the collagen content was 20 wt.%, the hydrogel composite was unable to form gel at 37 °C, but precipitated into white emulsion. In contrast, addition of 5 and 10 wt.% collagen retained gelling ability at 37 °C (Table 2 and Fig. 2). These two collagen concentrations were thus employed to form hydrogel composites. The addition of a small fraction of CS was found not to change gelling ability of the hydrogel composites. Gelation time was measured for the hydrogel composites. The time for a drop of 20 μl hydrogel composite solution to form an opaque gel was considered as a gelation time. Table 2 shows that the pure hydrogel and hydrogel composites were quickly gellable, where the pure hydrogel had a gelation time of 5 s, and the hydrogel composites exhibited a gelation time in the range of 4–6 s.

Hydrogel composite injectability was tested by injecting a 20 wt.%, 4 °C hydrogel composite solution through a 26-gauge needle. The hydrogel composite that can be injected through the needle was considered as being injectable. This injectability criterion was based on the consideration that applications such as myocardial and muscular injection employ needles as small as 26 gauge [37,38]. It was found that pure hydrogel and all the hydrogel composites were injectable (Fig. 2 and Table 2).

Hydrogel composites oxygen permeability was measured using EPR. Fig. 3 demonstrates that hydrogel composites were responsive to changes in oxygen concentration, indicating that they were oxygen permeable. The oxygen pressure in the hydrogel composites was ~159 mm Hg, similar to that in the air.

Water content in the hydrogel composites after gelation was dependent on collagen content (Table 2). In comparison with pure hydrogel, incorporation of 5% collagen significantly increased water content ($p < 0.05$). Further increase in collagen content to 10% only slightly increased water content. For hydrogel composite Tgel/Col5, the addition of CS was found to substantially decrease water content although there was no significant difference.

3.3. Hydrogel composites thermal properties

The hydrogel and hydrogel composites were stiff and brittle in dry state. DSC analysis demonstrated that glass transition temperature (T_g) of the hydrogel copolymer was 134.5 °C (Table 4, DSC curves are presented in Fig. S1 in Supplementary Information). The T_gs of the hydrogel composites were higher than that of the hydrogel copolymer, and increased with collagen content. Addition of CS into hydrogel composite was found to slightly increase T_g.

LCSTs of the hydrogel composites are presented in Table 4 (DSC curves are presented in Fig. S1 in Supplementary Information). All of the hydrogel composites possessed LCSTs around room temperature, ranging from 23.8 to 26.9 °C. The LCSTs were dependent on collagen content and CS addition. Table 4 shows that LCST increased with collagen content. For hydrogel composite Tgel/Col5, the addition of CS was seen to slightly increase LCST. The pure hydrogel was hydrolyzed in NaOH solution to remove the degradable side chain PTMC. The resulting polymer theoretically exhibits the same polymer structure as that completely degraded in PBS (Scheme 1). The hydrolyzed polymer possessed a LCST of 49.4 °C, which is well above 37 °C, demonstrating that the completely degraded polymer is soluble at body temperature.

3.4. Hydrogel composite mechanical properties

Fig. 2d and e shows that the hydrogel composite was stretchable at 37 °C. Quantitative mechanical properties under aqueous conditions at 37 °C were presented in Table 5. All the hydrogel composites were highly flexible with elongation greater than 1000%, exceeding strain range of the testing equipment. The tensile stresses and moduli were in the ranges of 10–17 kPa and 63–120 kPa, respectively. The tensile stress and modulus were related to collagen content and CS addition. The pure hydrogel possessed tensile stress and modulus of 16 ± 4 kPa and 63 ± 11 kPa, respectively. Addition of 5% collagen did not change tensile stress but significantly increased modulus to 100 ± 34 kPa ($p < 0.05$). When the collagen content was increased to 10%, the tensile stress was significantly decreased ($p < 0.05$) and the modulus was unchanged ($p > 0.05$). For Tgel/Col5 composite, addition of CS did not significantly alter both tensile stress and modulus.

3.5. Hydrogel composites degradation

In vitro degradation of pure hydrogel (Tgel), and hydrogel composites (Tgel/Col5 and Tgel/Col5/CS) in PBS at 37 °C is presented in

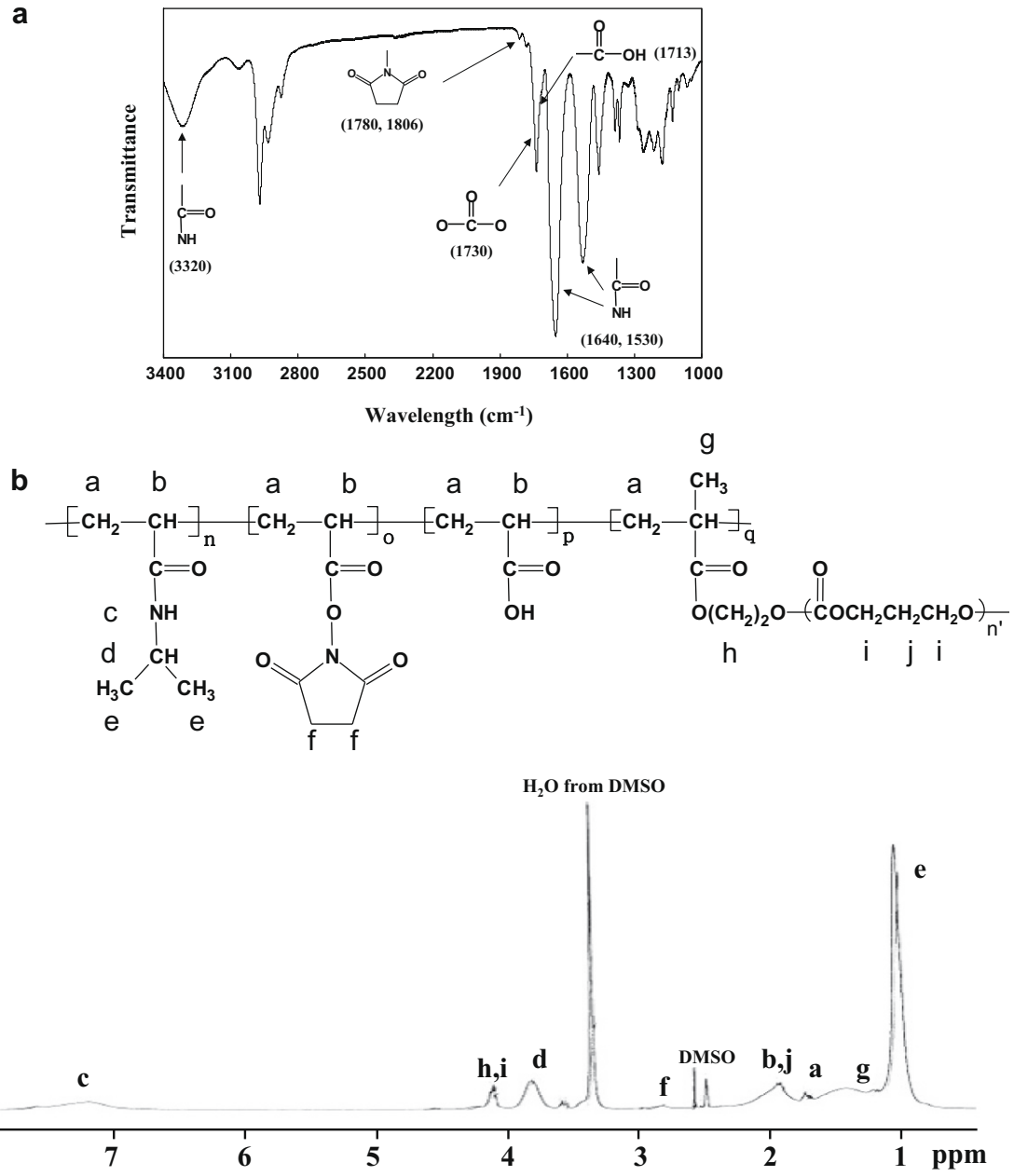

Fig. 1. Characterization of poly(NIPAAm-*co*-AAc-*co*-NAS-*co*-HEMAPTMC): (a) FTIR spectrum; (b) ^{1}H NMR spectrum.

Fig. 4. Both pure hydrogel and hydrogel composites demonstrated progressive mass loss during the degradation. After 14 days, they exhibited weight remaining ~90%. It was found that weight remaining of the Tgel at each time point was essentially equivalent to the Tgel/Col5 and Tgel/Col5/CS hydrogel composites. Comparing Tgel/Col5 and Tgel/Col5/CS, the addition of CS into the hydrogel composite did not significantly alter degradation rate.

To confirm degradability of the hydrogel, molecular weights of the hydrogel (Tgel) before and after degradation were measured by GPC. The number average molecular weight before degradation was 31,000 (PDI 1.72), which decreased to 20,000 (PDI 1.69) for the completely degraded hydrogel obtained by hydrolysis with NaOH, demonstrating that side chain PTMC was degradable.

Degradation products cytotoxicity was evaluated by examining cell viability of the NIH3T3 fibroblasts cultured in the medium containing different concentrations of completely degraded hydrogel copolymer. Fig. 5 demonstrates that the culture media containing 1–15 mg ml^{-1} degradation products had similar cell viability as the control medium without degradation products ($p > 0.05$). The cell viability was not significantly different among all concentrations ($p > 0.05$).

3.6. IGF-1 release kinetics

IGF-1 was loaded into both Tgel/Col5 and Tgel/Col5/CS to investigate the feasibility that the developed hydrogel composites can be used as vehicles for protein delivery. The concentration of IGF-1 in the collected release medium was measured by IGF-1 ELISA kit. Both hydrogel composites had encapsulation efficiencies greater than 90%. Fig. 6 presents the release kinetics of IGF-1 from both hydrogel composites. The IGF-1 demonstrated a two-stage release profile in the hydrogel composites during a 14-day release period, a fast release within the first 3 days and a slow release from days 3 to 14. The Tgel/Col5 exhibited significantly higher cumula-

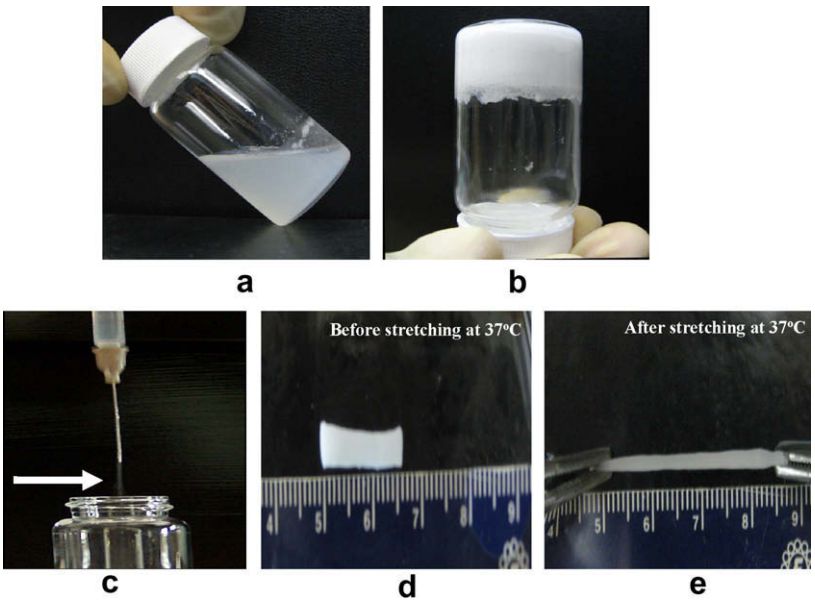

Fig. 2. Macroscopic images of the hydrogel composite (Tgel/Col5): (a) flowable at 4 °C; (b) formed gel at 37 °C; (c) injectable through 26-gauge needle at 4 °C; (d) gel before stretching at 37 °C; and (e) gel after stretching at 37 °C. Tgel and Col5 represent hydrogel copolymer and 5% collagen, respectively.

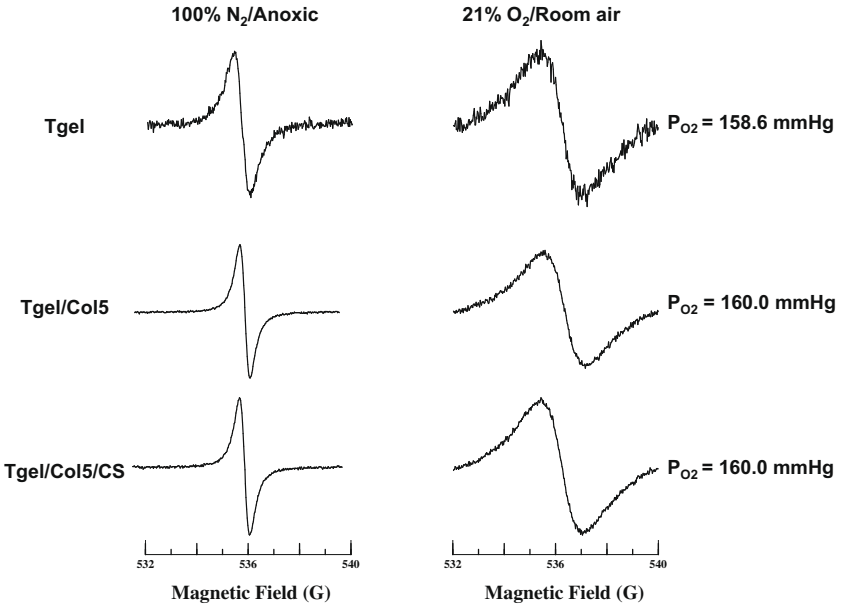

Fig. 3. EPR spectra of the hydrogel under N_2 and room temperature air (21% O_2). Hydrogel mixed with EPR sensitive probe LiNc-BuO was placed in a gas-permeable capillary tube, and flushed with 100% N_2 (anoxia) and room temperature air. Hydrogel showed a linear response to changes in oxygen concentration, illustrating its permeability to oxygen.

Table 4
Thermal properties of hydrogel composites.[a]

	T_g (°C)	LCST (°C)	
		Before degradation	After degradation
Tgel	134.5 ± 1.9	23.8 ± 0.6	49.4 ± 3.3
Tgel/Col5	135.3 ± 1.8	25.3 ± 0.1	–
Tgel/Col10	138.4 ± 1.4	26.9 ± 1.3	–
Tgel/Col5/CS	136.3 ± 0.2	26.1 ± 2.0	–

[a] Each T_g or LCST was obtained from three different measurements.

tive IGF-1 concentration than Tgel/Col5/CS at each time point ($p < 0.05$), indicating that CS addition significantly decreased IGF-1 release rate.

Table 5
Mechanical properties of hydrogel composites.

	Elongation (%)	Tensile stress (kPa)	Modulus (kPa)
Tgel	>1000	16 ± 4	63 ± 11
Tgel/Col5	>1000	16 ± 3	100 ± 34
Tgel/Col10	>1000	10 ± 1	120 ± 43
Tgel/Col5/CS	>1000	17 ± 2	100 ± 20

3.7. Bioactivity of released IGF-1

The bioactivity of released IGF-1 was assessed by quantifying NIH3T3 fibroblast growth after incubation with the collected

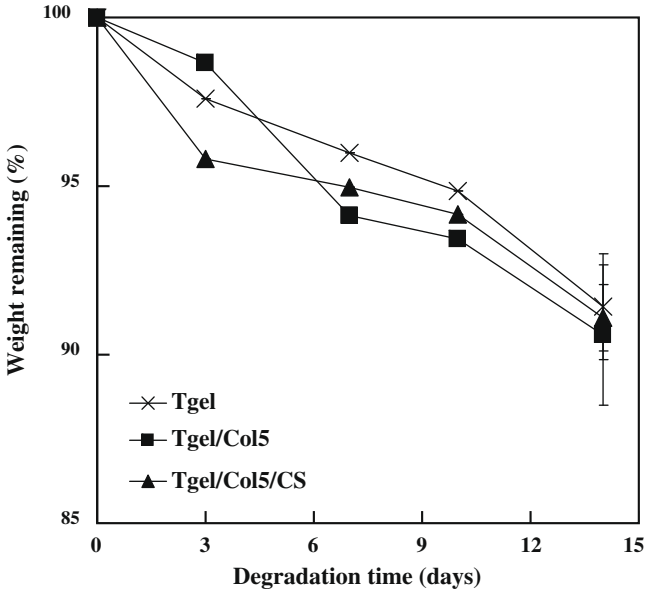

Fig. 4. Degradation of hydrogel (Tgel) and hydrogel composites (Tgel/Col5 and Tgel/Col5/CS) in PBS at 37 °C. Tgel, Col5 and CS represent hydrogel copolymer, 5% collagen and chondroitin sulfate, respectively.

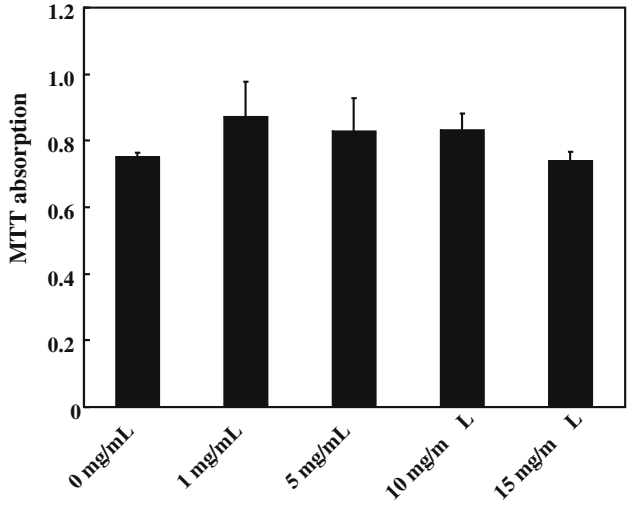

Fig. 5. Cytotoxicity of the hydrogel degradation products. NIH3T3 fibroblasts were cultured in the media containing different concentrations of degradation products. Cell viability was measured by MTT assay.

release medium for 48 h. To examine dose response of IGF-1 on cell growth, the release media containing 0, 1 and 10 ng ml^{-1} IGF-1 were used to culture cells. It was found that 1 ng ml^{-1} IGF-1 was sufficient to stimulate cell growth, and higher IGF-1 concentration showed greater stimulatory effect (Fig. 7). The bioactivity of IGF-1 released from hydrogel composites Tgel/Col5 and Tgel/Col5/CS are presented in Fig. 7. The Tgel/Col5 without IGF-1 loading was used as a negative control. The relative cell number for pure release medium, and release media incubated with hydrogel composite without IGF-1, was significantly lower than the release medium containing 1 ng ml^{-1} IGF-1. The IGF-1 released at each time point from each hydrogel composite was found to be bioactive, as the relative cell number for release media containing IGF-1 released at each time point was comparable or greater than that for the release medium containing 10 ng ml^{-1} IGF-1. The IGF-1 released from both hydrogel composites showed similar bioactivity during

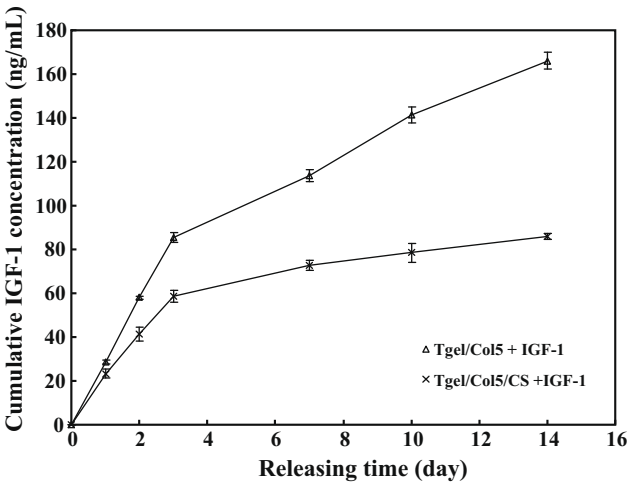

Fig. 6. Release kinetics of IGF-1 from hydrogel composites (Tgel/Col5 and Tgel/Col5/CS) at 37 °C. Tgel, Col5 and CS represent hydrogel copolymer, 5% collagen and chondroitin sulfate, respectively.

the first 3 days, but the Tgel/Col5 exhibited significantly higher bioactivity from day 3 to 14, in agreement with the release profiles shown in Fig. 6.

3.8. Cell adhesion on the hydrogel composite surfaces

MSCs were cultured on the hydrogel composite surfaces to evaluate their ability to support cell adhesion and the effect of IGF-1 loading on cell adhesion. Considering cell adhesion on the tissue culture plate surface to be 100%, the cell adhesion on the pure hydrogel (Tgel) surface was 51% (Fig. 8). Addition of 5% collagen in the hydrogel significantly increased cell adhesion. Both hydrogel composites (Tgel/Col5 and Tgel/Col5/CS) demonstrated similar cell adhesion as the tissue culture plate ($p > 0.1$). IGF-1 loading slightly increased cell adhesion, although there was no significant difference between the IGF-1 loaded and unloaded hydrogel composites.

3.9. MSC encapsulation and growth within hydrogel composites

MSCs were encapsulated in the hydrogel composites with or without IGF-1 to investigate the feasibility that the developed hydrogel composites can be used to encapsulate MSCs and to evaluate the effect of IGF-1 on MSC growth. MSCs were encapsulated into the hydrogel composites at a density of 2.5×10^6 cells ml^{-1}. The encapsulation efficiency was between 93% and 95% for all of the hydrogel composites. MSC encapsulation did not substantially change injectability and gelation time. The MSC encapsulated hydrogel composites remained to be injectable through a 26-gauge needle. The gelation time for MSC encapsulated hydrogel composites was 5 s (Table 2). The MSC encapsulated hydrogel composites retained high flexibility with elongation exceeding 1000%. In contrast, MSC encapsulation significantly decreased tensile stress and modulus (Fig. 9), where tensile stress decreased from 16 kPa to 10–12 kPa, and modulus decreased from 92–100 kPa to 60–73 kPa, respectively. No significant difference was found for MSC encapsulated Tgel/Col5 and Tgel/Col5/CS composites.

MSC growth in the hydrogel composites was quantified by cell number, which was counted after digestion with trypsin and dilution with PBS. Fig. 10 demonstrates that cell number increased during the culture for all of the hydrogel composites with or without IGF-1 loading. The cell number in IGF-1 loaded Tgel/Col5 was significantly higher than that in the non-IGF-1 loaded Tgel/Col5 at all time points ($p < 0.05$ for days 1, 3 and 7). The IGF-1 loaded

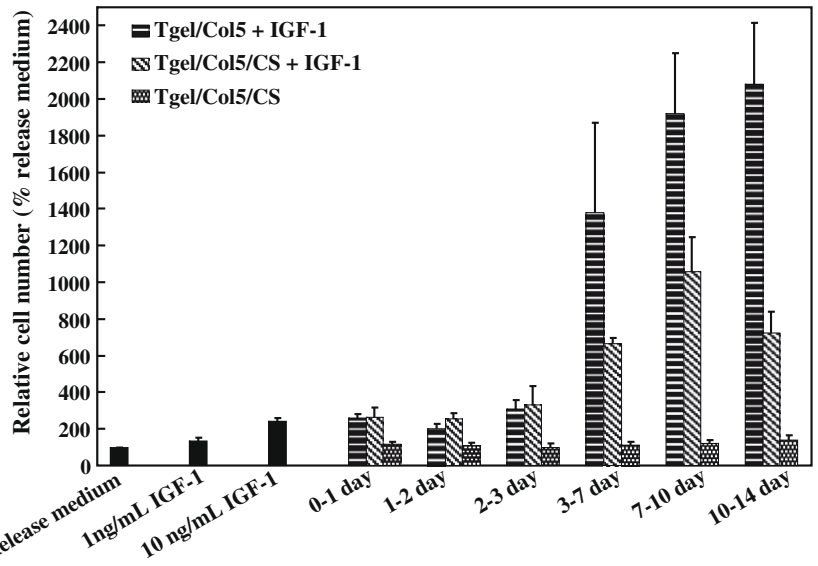

Fig. 7. Bioactivity of released IGF-1 from Tgel/Col5 and Tgel/Col5/CS. The release media containing 0, 1 and 10 ng ml^{-1} IGF-1 were used as controls. Tgel, Col5 and CS represent hydrogel copolymer, 5% collagen and chondroitin sulfate, respectively.

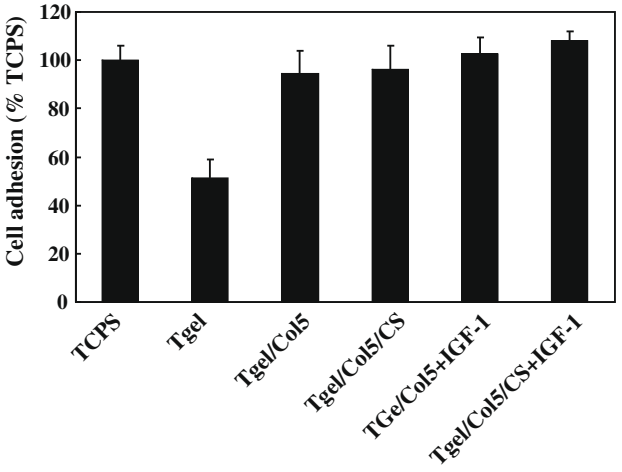

Fig. 8. Human MSC adhesion on the surface of hydrogel (Tgel) and hydrogel composites (Tgel/Col5 and Tgel/Col5/CS) with or without IGF-1 loading. Tgel, Col5 and CS represent hydrogel copolymer, 5% collagen and chondroitin sulfate, respectively.

Tgel/Col5/CS had similar cell number as non-IGF-1 loaded Tgel/Col5/CS at day 1 and 3. However, at day 7, the IGF-1 loaded Tgel/Col5/CS had significantly higher cell number than non-IGF-1 loaded Tgel/Col5/CS ($p < 0.05$).

Live cell staining showed that MSCs in hydrogel composites with or without IGF-1 loading were alive during the 7-day culture period (Fig. 11). For each hydrogel composite, the cell density was seen to increase during the culture. At day 7, the IGF-1 loaded composites had obviously higher cell density as compared with their non-loaded counterparts.

Fig. 12 shows the expression of osteogenic and adipogenic markers in MSCs encapsulated hydrogel composites with or without IGF-1 loading. MSCs cultured on the tissue culture plate were used as control. After 7 days of culture, MSCs encapsulated in the hydrogel composites with and without IGF-1 expressed collagen I, osteonectin and PPARγ2, which were also expressed in MSCs cultured on the tissue culture plate.

4. Discussion

Stem (progenitor) cell therapy has been applied to treat various diseases such as acute and chronic myocardial infarction [39–41] and muscular dysfunction [42,43]. Traditional cell therapy utilizes an approach that directly injects cell suspension into target tissues. This approach is easily applicable to tissues like skeletal muscle as they are relatively static during the injection [43]. For those

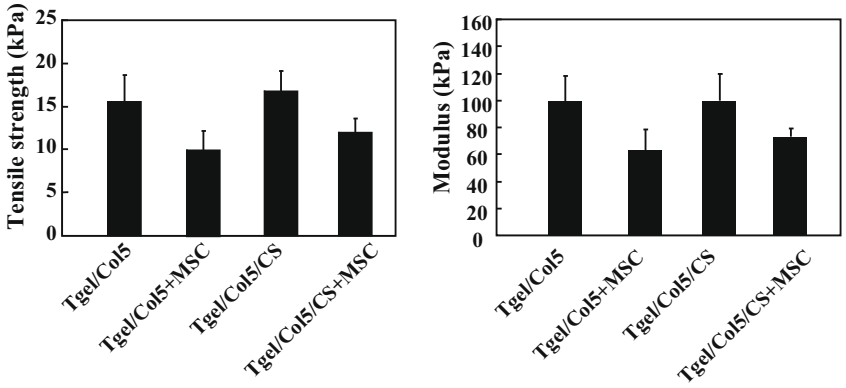

Fig. 9. Tensile mechanical properties of MSC encapsulated hydrogel composites (Tgel/Col5 and Tgel/Col5/CS). Tgel, Col5 and CS represent hydrogel copolymer, 5% collagen and chondroitin sulfate, respectively. MSC encapsulation density was 2.5×10^6 cells ml^{-1}.

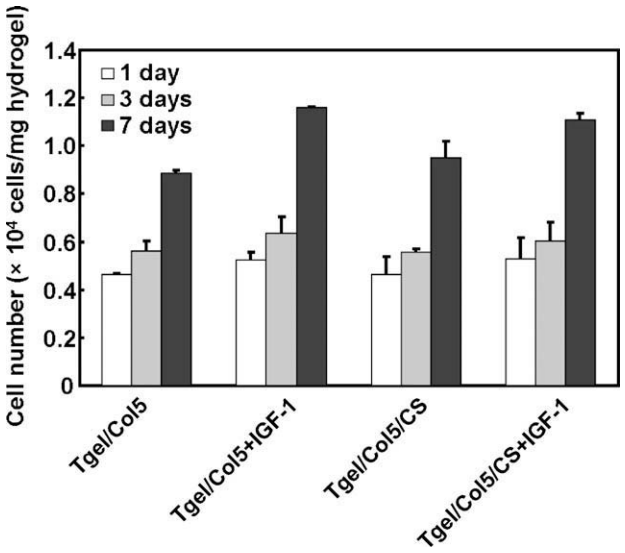

Fig. 10. Human MSC growth in hydrogel composites (Tgel/Col5 and Tgel/Col5/CS) with or without IGF-1 loading. MSC encapsulation density was 2.5×10^6 cells ml^{-1}. Cell number was counted after digestion with trypsin/EDTA and diluting with PBS.

actively mobile tissues such as heart, the major issue associated with cell injection is cell retention. Significant fractions of cells were found to leak or wash out during the injection, owing to low viscosity of the cell suspension [44,45]. Inferior cell engraftment rate is another issue for cell injection. It has been shown that cell engraftment rate is usually in the range of 0–0.3% a few weeks after myocardium injection [46,47]. This is mainly attributed to poor nutrition supply in an infarcted heart and the retained cells lack of an anchoring matrix, resulting in apoptosis [48]. To overcome these issues, injectable biomaterials have been used as cell carriers [44]. Injectable biomaterials not only increase cell retention as a result of higher viscosity of the cell suspension, but also provide matrices for cells to anchor for reducing apoptosis. In addition, the injectable biomaterials protect cells from direct attack by body's immune system, provide a microenvironment for stem (progenitor) cell differentiation, and provide a mechanical support to the diseased tissue. Fibrin [47–49] collagen [50], matrigel [51], self-assembling peptides [52], chitosan [53] and alginate [54] have been utilized as cell carriers. The major disadvantages of these carriers lie in fast degradation, slow gelation rate and inferior mechanical properties. The fast degradation allows biomaterials to be quickly cleared away in vivo, leading to a loss of protective microenvironment for cells and a loss of mechanical support to the target tissue. The injectable biomaterials with inferior mechanical properties are unable to respond synchronically with the tissue motion, and therefore cannot effectively transfer mechanical stimuli from the tissue environment to the cells to regenerate mechanically functional tissues. When injecting biomaterials into the actively mobile tissues, fast gelation rate is often desired as the slow gelation rate biomaterials may raise the possibility of blocking blood flow and lead to tissue necrosis [55].

The objective of this work was to develop injectable hydrogels addressing above limitations and being suitable for delivering stem (progenitor) cells into actively mobile soft tissues like heart. Towards this goal, we have developed a family of thermosensitive hydrogel composites that were readily injectable at low temperature, were capable of rapidly gelling (<6 s), were highly flexible at body temperature, degraded at a rate of ~5 wt.% week^{-1}, and were able to release cell prosurvival growth factor and support cell adhesion and growth. The hydrogel composites were formed by mixing degradable PNIPAAm based hydrogel with collagen. The hydrogel was synthesized based on monomer units of NIPAAm, AAc, NAS and degradable HEMAPTMC (Fig. 1b). The role of NIPAAm was to impart polymer with thermosensitivity. The AAC was used to increase solubility of the hydrogel. It can also increase hydrophilicity of the hydrogel following degradation of side chain PTMC, and allow its LCST to be higher than 37 °C so that it can dissolve in the water at normal body temperature [56,57]. The introduction of hydrophobic and degradable HEMAPTMC was to increase hydrophobicity of the hydrogel and decrease its LCST to well below body temperature, so that gelation could occur at 37 °C before degrada-

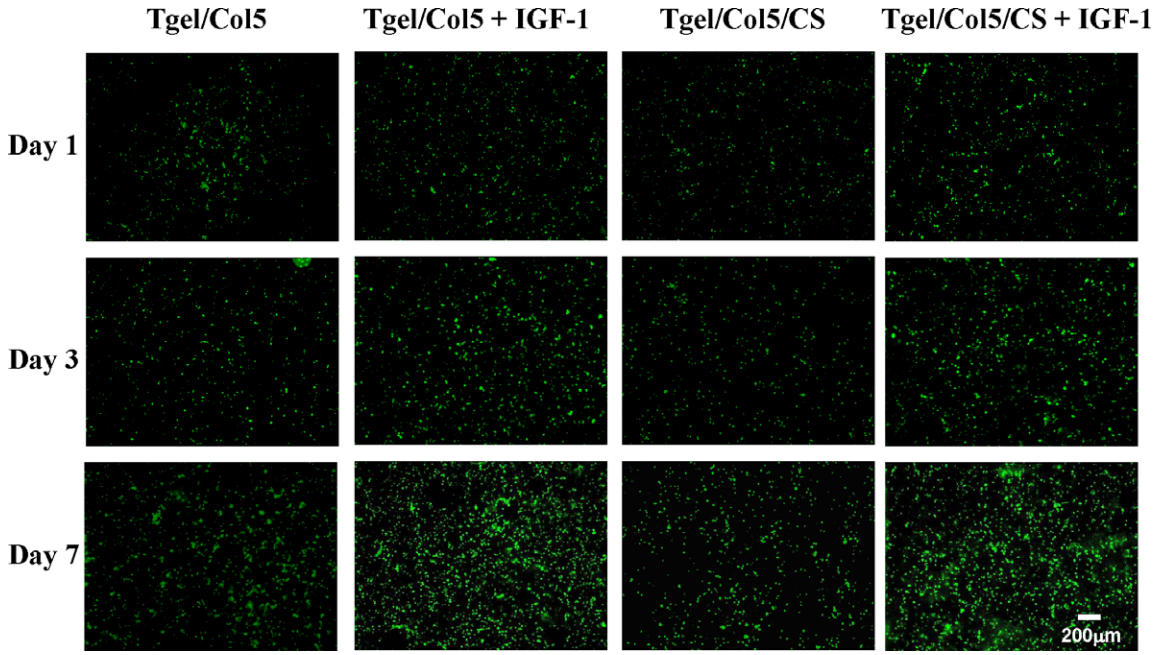

Fig. 11. Fluorescent images of live MSCs grown in hydrogel composites (Tgel/Col5 and Tgel/Col5/CS) with or without IGF-1 loading. MSC encapsulation density was 2.5×10^6 cells ml^{-1}. MSCs were labeled with live cell stain CMFDA.

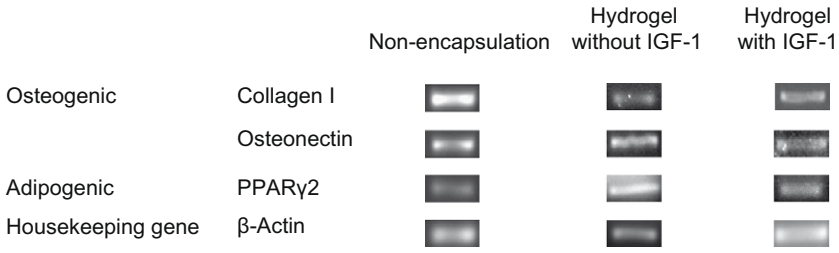

Fig. 12. Gene expression of osteogenic and adipogenic markers of MSCs encapsulated in the hydrogel composites with or without IGF-1 loading, and cultured in the tissue culture plate (non-encapsulation). Note that these genes were selected to confirm MSC multipotency.

tion [58]. Table 4 and Fig. 2 demonstrated that the hydrogel was able to gel at 37 °C before degradation and the completely degraded hydrogel copolymer was soluble at 37 °C as its LCST was well above 37 °C (49.4 °C). The introduction of NAS was to enable the hydrogel to conjugate with biomolecules such as collagen to form composites [11]. Collagen is a major ECM in the tissues serving as an anchoring matrix for cells and a reservoir for biomolecules such as growth factors. Incorporating collagen in the composites was aimed at improving hydrogel biocompatibility, and providing binding sites for growth factors that may impart composites with bioactivity. CS was also introduced into the hydrogel composites. CS is one of the major glycosaminoglycans in the extracellular matrix. It functions to bind and modulate growth factors and cytokines, and inhibit proteases. It is also involved in the adhesion, migration, proliferation and differentiation of cells [59].

The hydrogel composites were fabricated based on the hydrogel and collagen. Two forms of collagen may exist within the hydrogel composites, i.e. conjugated collagen resulting from reaction of NHS groups in the hydrogel with amine groups in the collagen; and physically entangled collagen. DSC results based on dry composites showed that collagen addition increased T_g of the hydrogel copolymer (Table 2), largely attributing to hydrogen bond interaction between PNIPAAm and collagen. The T_g was further increased as the CS was added into the composite. This is possible a result that CS incorporation enhanced hydrogen bond interaction with PNIPAAm. The hydrogel and hydrogel composites possessed LCSTs around room temperature, allowing them to form gels at body temperature. Collagen incorporation increased hydrogel hydrophilicity as can be seen that water contents of hydrogel composites were higher than that of the pure hydrogel (Table 2). Table 4 demonstrated that LCSTs of the hydrogel composites increased with collagen content. LCST is related to the hydrogel composite hydrophilicity, where higher hydrophilicity would have greater inhibiting effect on the dehydration of polymer chain during the gelation process and result in higher LCSTs [11]. Addition of small fraction of CS increased LCST of the hydrogel composite although it slightly decreased water content. This is probably due to the negatively charged carboxylic and sulfate groups in the CS enhanced the inhibiting effect on polymer chain dehydration. Previous work demonstrated that ionic interaction played critical role in inhibiting dehydration of the polymer chain [11].

All of the hydrogel composites were injectable through small 26-gauge needles. Encapsulation of MSCs at a density of 2.5×10^6 cells ml^{-1} was found not to affect injectability (Table 2). This is attractive as it would allow the hydrogel composites with or without cells to be delivered into tissues such as myocardium without causing substantial damage [60]. The hydrogel composites with or without combining with cells exhibited fast gelation rate, mostly gelled within 6 s. The high gelation rate hydrogels may be desirable for tissues such as myocardium, where high density of capillaries and vasculatures is present, as it would decrease the possibility for the injected hydrogel to block the blood flow leading to tissue necrosis. The hydrogel composites were oxygen permeable, which may facilitate survival and growth of the cells encapsulated within the hydrogel.

The hydrogel composites exhibited attractive mechanical properties. All of the hydrogel composites were highly flexible with elongation higher than 1000%, tensile stresses ranging from 10 to 17 kPa and moduli ranging from 63 to 120 kPa. The tensile stress and modulus were related to collagen content and CS addition. Addition of 5% collagen in the hydrogel composite did not significantly alter tensile stress, while addition of 10% collagen did (Table 5). This decrease is largely attributed to the decrease of relative content of hydrogel, and the hydrogel had higher tensile stress than collagen gel [61]. Addition of small fraction of CS into the hydrogel composite did not significantly change mechanical properties. These tensile properties including elongation and moduli are greater than those of collagen gel [62], fibrin [62,63], chitosan [64], alginate [65] and polyvinyl alcohol (PVA) hydrogels [66]. These flexible hydrogel composites may be suitable for engineering mechano-active soft tissues as they would allow effective mechanical stimulus transfer during the tissue regeneration in vivo. The moduli of the hydrogel composites were similar to those of the rat and human myocardium (1–140 kPa for rat myocardium, and 20–500 kPa for human myocardium) [67]. Previous theoretical modeling of myocardium injection demonstrated that material modulus plays an important role in decreasing wall stress of the infarcted myocardium [68]. It is hypothesized that injection of materials with matched moduli as the myocardium would effectively decrease wall stress and attenuate myocardial remodeling [68]. Furthermore, injection of these hydrogel composites with stem (progenitor) cells may provide a native-like mechanical environment for cells to differentiate into appropriate cell types for enhanced tissue regeneration.

The hydrogel and hydrogel composites experienced gradual weight loss during a 2-week period, with weight loss less than 10% (Fig. 4). Collagen and CS addition did not significantly change degradation properties. Under current degradation conditions, hydrolysis of side chain PTMC dominated degradation since no enzyme was presented. It is expected that the hydrogel composites would experience faster degradation in vivo as both hydrolysis and enzymatic degradation would occur. Current hydrogel and hydrogel composites had much slower degradation rate than our previously developed biodegradable and thermosensitive hydrogel using PLA as a degradable segment, which showed weight losses between 60% and 90% within 14 days. This might result from slow degradation characteristic of PTMC [69]. The degradation products were found to be non-toxic as they did not affect NIH3T3 fibroblast growth, even at the concentration of 15 mg ml^{-1} (Fig. 5).

IGF-1 was encapsulated into the hydrogel composites in order to improve survival and growth of the encapsulated cells. IGF-1 is a prosurvival growth factor for many cell types including smooth muscle cell, cardiomyocyte and MSC [70–72]. The hydrogel composites were able to maintain a sustained release of bioactive IGF-1 during the 2-week release period (Figs. 6 and 7). A two-stage

release profile was found: a fast release during the first 3 days, and a slower release afterwards. The fast release may be dominated by both IGF-1 diffusion and hydrogel composite degradation. The slower release may be attributed to hydrogel composite degradation. Comparing the release kinetics of Tgel/Col5 and Tgel/Col5/CS, it was found that Tgel/Col5 had a significantly higher release rate at any time interval, indicating that small fraction of CS was able to adjust IGF-1 release kinetics. This may be explained by water content of the hydrogel composites and interactions between IGF-1 and CS. Table 2 demonstrates that Tgel/Col5 possessed higher water content than Tgel/Col5/CS. This higher water content may allow IGF-1 to diffuse out of the hydrogel composite easier. In addition, strong interactions between CS and IGF-1 may attenuate IGF-1 release. CS is consisted of negatively charges (carboxylic and sulfate) that may form strong interactions with amine groups in the IGF-1.

MSCs were cultured on the surfaces of the hydrogel composites to evaluate cell adhesion. Pure hydrogel was found not to support extensive cell adhesion, mainly due to its high hydrophilicity. Addition of cell adhesive collagen within the hydrogel significantly improved cell adhesion comparable to TCPS (Fig. 8). IGF-1 loading did not significantly improve cell adhesion. MSCs were further encapsulated into the hydrogel composites to evaluate their survival/growth in the 3D environment. Figs. 10 and 11 show that MSCs could proliferate in all the hydrogel composites with or without IGF-1 loading. The IGF-1 loaded hydrogel composites exhibited higher cell number than those non-IGF-1 loaded hydrogel composites after 7 days' culture, resulting from stimulatory effect of IGF-1. These results further demonstrated that the IGF-1 within the hydrogel composites was bioactive. MSCs cultured in the hydrogel composites with or without IGF-1 expressed osteogenic and adipogenic markers after 7 days of culture. This suggests that the hydrogel composite microenvironment is capable of maintaining MSC multipotency [73] and IGF-1 loading could not induce MSC differentiation. These results suggest that current hydrogel composites with IGF-1 loading may be used as effective cell carriers for cardiovascular tissue engineering. MSC have been widely used for heart injection. The combination of MSC with hydrogel composites and IGF-1 may enhance its therapeutic effect. It is also possible that growth factors with different simulative effects be loaded within the hydrogel composites. For example, angiogenic growth factors like VEGF and bFGF may be applied for fast angiogenesis in vivo, as the released growth factor may stimulate blood vessel formation around the hydrogel, while the growth factor inside may stimulate MSC differentiation into endothelial cells [74].

5. Conclusions

We have developed a family of highly flexible hydrogel composites based on collagen, chondroitin sulfate and a thermosensitive and degradable poly(*N*-isopropylacrylamide) copolymer. The hydrogel composites exhibited attractive injectability, gelation properties, oxygen permeability and mechanical properties. The hydrogel composites were capable of releasing bioactive IGF-1 during a 2-week period. The IGF-1 loading accelerated MSC growth within in the 3D hydrogel composites. These hydrogel composites may be used as growth factor and cell carriers for cardiovascular tissue engineering.

Acknowledgements

The authors thank Dr John Lannutti for help on mechanical properties characterization. We are grateful to Dr Zuwei Ma in McGowan Institute for Regenerative Medicine at the University of Pittsburgh for conducting molecular weight measurements. This work was funded by Institute for Materials Research at the Ohio State University.

Appendix A. Supplementary data

Supplementary data associated with this article can be found, in the online version, at doi:10.1016/j.actbio.2009.12.011.

Appendix B. Figures with essential colour discrimination

Certain figures in this article, particularly Figures 2, 11 and Scheme 2, are difficult to interpret in black and white. The full colour images can be found in the on-line version, at doi: 10.1016/j.actbio.2009.12.011.

References

[1] Pedersen JA, Swartz MA. Mechanobiology in the third dimension. Ann Biomed Eng 2005;33(11):1469–90.
[2] Engler AJ, Sen S, Sweeney HL, Discher DE. Matrix elasticity directs stem cell lineage specification. Cell 2006;126(4):677–89.
[3] Baroli B. Hydrogels for tissue engineering and delivery of tissue-inducing substances. J Pharm Sci 2007;96(9):2197–223.
[4] Nicodemus GD, Bryant SJ. Cell encapsulation in biodegradable hydrogels for tissue engineering applications. Tissue Eng B Rev 2008;14(2):149–65.
[5] Carbonetto ST, Gruver MM, Turner DC. Nerve fiber growth on defined hydrogel substrates. Science 1982;216(4548):897–9.
[6] Yu L, Ding J. Injectable hydrogels as unique biomedical materials. Chem Soc Rev 2008;37(8):1473–81.
[7] Van Tomme SR, Storm G, Hennink WE. In situ gelling hydrogels for pharmaceutical and biomedical applications. Int J Pharm 2008;355(1–2):1–18.
[8] Aliyar HA, Hamilton PD, Ravi N. Refilling of ocular lens capsule with copolymeric hydrogel containing reversible disulfide. Biomacromolecules 2005;6(1):204–11.
[9] Holland TA, Tabata Y, Mikos AG. Dual growth factor delivery from degradable oligo(poly(ethylene glycol) fumarate) hydrogel scaffolds for cartilage tissue engineering. J Control Release 2005;101(1–3):111–25.
[10] Guo X, Park H, Liu G, Liu W, Cao Y, Tabata Y, et al. In vitro generation of an osteochondral construct using injectable hydrogel composites encapsulating rabbit marrow mesenchymal stem cells. Biomaterials 2009;30(14):2741–52.
[11] Guan J, Hong Y, Ma Z, Wagner WR. Protein-reactive, thermoresponsive copolymers with high flexibility and biodegradability. Biomacromolecules 2008;9(4):1283–92.
[12] Hennink WE, van Nostrum CF. Novel crosslinking methods to design hydrogels. Adv Drug Deliv Rev 2002;54(1):13–36.
[13] Nguyen KT, West JL. Photopolymerizable hydrogels for tissue engineering applications. Biomaterials 2002;23(22):4307–14.
[14] Jeong B, Kim SW, Bae YH. Thermosensitive sol–gel reversible hydrogels. Adv Drug Deliv Rev 2002;54(1):37–51.
[15] Tate MC, Shear DA, Hoffman SW, Stein DG, LaPlaca MC. Biocompatibility of methylcellulose-based constructs designed for intracerebral gelation following experimental traumatic brain injury. Biomaterials 2001;22(10):1113–23.
[16] Ruel-Gariepy E, Leroux JC. In situ-forming hydrogels – review of temperature-sensitive systems. Eur J Pharm Biopharm 2004;58(2):409–26.
[17] Jeong B, Bae YH, Lee DS, Kim SW. Biodegradable block copolymers as injectable drug-delivery systems. Nature 1997;388(6645):860–2.
[18] Raucher D, Massodi I, Bidwell GL. Thermally targeted delivery of chemotherapeutics and anti-cancer peptides by elastin-like polypeptide. Expert Opin Drug Deliv 2008;5(3):353–69.
[19] Chilkoti A, Dreher MR, Meyer DE, Raucher D. Targeted drug delivery by thermally responsive polymers. Adv Drug Deliv Rev 2002;54(5):613–30.
[20] Shimizu T, Yamato M, Isoi Y, Akutsu T, Setomaru T, Abe K, et al. Fabrication of pulsatile cardiac tissue grafts using a novel 3-dimensional cell sheet manipulation technique and temperature-responsive cell culture surfaces. Circ Res 2002;90(3):e40–8.
[21] Takeda N, Nakamura E, Yokoyama M, Okano T. Temperature-responsive polymeric carriers incorporating hydrophobic monomers for effective transfection in small doses. J Control Release 2004;95(2):343–55.
[22] Klouda L, Mikos AG. Thermoresponsive hydrogels in biomedical applications. Eur J Pharm Biopharm 2008;68(1):34–45.
[23] Li F, Carlsson D, Lohmann C, Suuronen E, Vascotto S, Kobuch K, et al. Cellular and nerve regeneration within a biosynthetic extracellular matrix for corneal transplantation. Proc Natl Acad Sci USA 2003;100(26):15346–51.
[24] Guan J, Wagner WR, Fujimoto KL. Thermoresponsive, biodegradable, elastomeric material. US Patent No. 0096975A1; 2008.
[25] Guan J, Hong Y, Ma Z, Wagner WR. Protein-reactive, injectable, thermosensitive and flexible hydrogels. 2008 World Congress of Biomaterials (#1776). Amsterdam; 2008.

[26] Lee JE, Kim KE, Kwon IC, Ahn HJ, Lee SH, Cho HC, et al. Effects of the controlled-released TGF-beta 1 from chitosan microspheres on chondrocytes cultured in a collagen/chitosan/glycosaminoglycan scaffold. Biomaterials 2004;25(18):4163–73.
[27] Pieper JS, van Wachem PB, van Luyn MJA, Brouwer LA, Hafmans T, Veerkamp JH, van Kuppevelt TH. Attachment of glycosaminoglycans to collagenous matrices modulates the tissue response in rats. Biomaterials 2000;21: 1689–99.
[28] Pandian RP, Parinandi NL, Ilangovan G, Zweier JL, Kuppusamy P. Novel particulate spin probe for targeted determination of oxygen in cells and tissues. Free Radic Biol Med 2003;35(9):1138–48.
[29] Khan M, Kutala VK, Vikram DS, Wisel S, Chacko SM, Kuppusamy ML, et al. Skeletal myoblasts transplanted in the ischemic myocardium enhance in situ oxygenation and recovery of contractile function. Am J Physiol Heart Circ Physiol 2007;293(4):H2129–39.
[30] Kutala VK, Parinandi NL, Pandian RP, Kuppusamy P. Simultaneous measurement of oxygenation in intracellular and extracellular compartments of lung microvascular endothelial cells. Antioxid Redox Signal 2004;6(3):597–603.
[31] Elvira C, Mano JF, San Román J, Reis RL. Starch-based biodegradable hydrogels with potential biomedical applications as drug delivery systems. Biomaterials 2002;23(9):1955–66.
[32] Reddy TT, Kano A, Maruyama A, Hadano M, Takahara A. Thermosensitive transparent semi-interpenetrating polymer networks for wound dressing and cell adhesion control. Biomacromolecules 2008;9(4):1313–21.
[33] Guan J, Stankus JJ, Wagner WR. Biodegradable elastomeric scaffolds with basic fibroblast growth factor release. J Control Release 2007;120(1–2):70–8.
[34] Tanihara M, Suzuki Y, Yamamoto E, Noguchi A, Mizushima Y. Sustained release of basic fibroblast growth factor and angiogenesis in a novel covalently crosslinked gel of heparin and alginate. J Biomed Mater Res 2001;56(2): 216–21.
[35] Du J, Cai SH, Suzuki H, Akhand AA, Ma XY, Takagi Y, et al. Involvement of MEKK1/ERK/P21(Waf1/Cip1) signal transduction pathway in inhibition of IGF-I-mediated cell growth response by methylglyoxal. J Cell Biochem 2003;88(6):1235–46.
[36] Yow SZ, Quek CH, Yim KF, Lim CT, Leong KW. Collagen-based fibrous scaffold for spatial organization of encapsulated and seeded human mesenchymal stem cells. Biomaterials 2009;30:1133–42.
[37] Song L, Webb NE, Song Y, Tuan RS. Identification and functional analysis of candidate genes regulating mesenchymal stem cell self-renewal and multipotency. Stem Cells 2006;24(7):1707–18.
[38] Yu J, Gu Y, Du KT, Mihardja S, Sievers RE, Lee RJ. The effect of injected RGD modified alginate on angiogenesis and left ventricular function in a chronic rat infarct model. Biomaterials 2009;30(5):751–6.
[39] Cho MH, Kim KS, Ahn HH, Kim MS, Kim SH, Khang G, et al. Chitosan gel as an in situ-forming scaffold for rat bone marrow mesenchymal stem cells in vivo. Tissue Eng A 2008;14(6):1099–108.
[40] Ma J, Ge J, Zhang S, Sun A, Shen J, Chen L, et al. Time course of myocardial stromal cell-derived factor 1 expression and beneficial effects of intravenously administered bone marrow stem cells in rats with experimental myocardial infarction. Basic Res Cardiol 2005;100(3):217–23.
[41] Shake JG, Gruber PJ, Baumgartner WA, Senechal G, Meyers J, Redmond JM, et al. Mesenchymal stem cell implantation in a swine myocardial infarct model: engraftment and functional effects. Ann Thorac Surg 2002;73(6):1919–25.
[42] Toma C, Pittenger MF, Cahill KS, Byrne BJ, Kessler PD. Human mesenchymal stem cells differentiate to a cardiomyocyte phenotype in the adult murine heart. Circulation 2002;105(1):93–8.
[43] Sacco A, Doyonnas R, Kraft P, Vitorovic S, Blau HM. Self-renewal and expansion of single transplanted muscle stem cells. Nature 2008;456(7221):502–6.
[44] Nozaki M, Li Y, Zhu J, Ambrosio F, Uehara K, Fu FH, et al. Improved muscle healing after contusion injury by the inhibitory effect of suramin on myostatin, a negative regulator of muscle growth. Am J Sports Med 2008;36(12): 2354–62.
[45] Christman KL, Lee RJ. Biomaterials for the treatment of myocardial infarction. J Am Coll Cardiol 2006;48(5):907–13.
[46] Reffelmann T, Kloner RA. Cellular cardiomyoplasty – cardiomyocytes, skeletal myoblasts, or stem cells for regenerating myocardium and treatment of heart failure? Cardiovasc Res 2003;58(2):358–68.
[47] Radosevich JA, Haines GK, Elseth KM, Shambaugh 3rd GE, Maker VK. A new method for the detection of viable cells in tissue sections using 3-[4,5-dimethylthiazol-2-yl]-2,5-diphenyltetrazolium bromide (MTT): an application in the assessment of tissue damage by surgical instruments. Virchows Arch B Cell Pathol Incl Mol Pathol 1993;63(6):345–50.
[48] Zhang G, Hu Q, Braunlin EA, Suggs LJ, Zhang J. Enhancing efficacy of stem cell transplantation to the heart with a PEGylated fibrin biomatrix. Tissue Eng A 2008;14(6):1025–36.
[49] Nuttelman CR, Tripodi MC, Anseth KS. Synthetic hydrogel niches that promote hMSC viability. Matrix Biol 2005;24(3):208–18.
[50] Ryu JH, Kim IK, Cho SW. Implantation of bone marrow mononuclear cells using injectable fibrin matrix enhances neovascularization in infarcted myocardium. Biomaterials 2005;26(3):319–26.
[51] Thompson CA, Nasseri BA, Makower J. Percutaneous transvenous cellular ardiomyoplasty. A novel nonsurgical approach for myocardial cell transplantation. J Am Coll Cardiol 2003;41(11):1964–71.
[52] Kofidis T, de Bruin JL, Hoyt G. Injectable bioartificial myocardial tissue for large-scale intramural cell transfer and functional recovery of injured heart muscle. J Thorac Cardiovasc Surg 2004;128(4):571–8.
[53] Davis ME, Motion JP, Narmoneva DA. Injectable self-assembling peptide nanofibers create intramyocardial microenvironments for endothelial cells. Circulation 2005;111(4):442–50.
[54] Yeo Y, Geng WL, Ito T, et al. Photocrosslinkable hydrogel for myocyte cell culture and injection. J Biomed Mater Res B Appl Biomater 2007;81(2):312–22.
[55] Tsur-Gang O, Ruvinov E, Landa N, Holbova R, Feinberg MS, Leor J, et al. The effects of peptide-based modification of alginate on left ventricular remodeling and function after myocardial infarction. Biomaterials 2009;30(2):189–95.
[56] Wang T, Wu DQ, Jiang XJ, Zhang XZ, Li XY, Zhang JF, et al. Novel thermosensitive hydrogel injection inhibits post-infarct ventricle remodeling. Eur J Heart Fail 2009;11(1):14–9.
[57] Lee BH, Vernon B. In situ-gelling, erodible *N*-isopropylacrylamide copolymers. Macromol Biosci 2005;5(7):629–35.
[58] Kim S, Healy KE. Synthesis and characterization of injectable poly(*N*-isopropylacrylamide-co-acrylic acid) hydrogels with proteolytically degradable cross-links. Biomacromolecules 2003;4(5):1214–23.
[59] Neradovic D, Soga O, Van Nostrum CF, Hennink WE. The effect of the processing and formulation parameters on the size of nanoparticles based on block copolymers of poly(ethylene glycol) and poly(*N*-isopropylacrylamide) with and without hydrolytically sensitive groups. Biomaterials 2004;25(12):2409–18.
[60] Aoki M, Morishita R, Higaki J, Moriguchi A, Kida I, Hayashi S, et al. *In vivo* transfer efficiency of antisense oligonucleotides into the myocardium using HVJ–liposome method. Biochem Biophys Res Commun 1997;231(3):540–5.
[61] Elbjeirami WM, Yonter EO, Starcher BC, West JL. Enhancing mechanical properties of tissue-engineered constructs via lysyl oxidase crosslinking activity. J Biomed Mater Res A 2003;66(3):513–21.
[62] Wen Q, Basu A, Winer JP, Yodh AG, Janmey PA. Local, global deformations in a strain-stiffening fibrin gel. New J Phys 2007;9:428.
[63] Janmey PA, Mccormick ME, Rammensee S, Leight JL, Georges PC, MacKintosh FC. Negative normal stress in semiflexible biopolymer gels. Nat Mater 2007;6(1):48–51.
[64] Chen JP, Cheng TH. Preparation and evaluation of thermo-reversible copolymer hydrogels containing chitosan and hyaluronic acid as injectable cell carriers. Polymer 2009;50(1):107–16.
[65] Vallée F, Müller C, Durand A, Schimchowitsch S, Dellacherie E, Kelche C, et al. Synthesis and rheological properties of hydrogels based on amphiphilic alginate-amide derivatives. Carbohydr Res 2009;344(2):223–8.
[66] Schmedlen RH, Masters KS, West JL. Photocrosslinkable polyvinyl alcohol hydrogels that can be modified with cell adhesion peptides for use in tissue engineering. Biomaterials 2002;23(22):4325–32.
[67] Chen QZ, Harding SE, Ali NN, Lyon AR, Boccaccini AR. Biomaterials in cardiac tissue engineering: ten years of research survey. Mater Sci Eng R 2008;59(1):1–37.
[68] Wall ST, Walker JC, Healy KE, Ratcliffe MB, Guccione JM. Theoretical impact of the injection of material into the myocardium: a finite element model simulation. Circulation 2006;114(24):2627–35.
[69] Pego AP, van Luyn MJA, Brouwer LA, van Wachem PB, Poot AA, Grijpma DW, et al. In vivo behavior of poly(1,3-trimethylene carbonate) and copolymers of 1,3-trimethylene carbonate with D,L-lactide or epsilon-caprolactone: degradation and tissue response. J Biomed Mater Res A 2003;67:1044–54.
[70] Huang YC, Khait L, Birla RK. Modulating the functional performance of bioengineered heart muscle using growth factor stimulation. Ann Biomed Eng 2008;36:1372–82.
[71] Laviola L, Natalicchio A, Giorgino F. The IGF-I signaling pathway. Curr Pharm Des 2007;13(7):663–9.
[72] Opgaard OS, Wang PH. IGF-I is a matter of heart. Growth Horm IGF Res 2005;15(2):89–94.
[73] Yow SZ, Quek CH, Yim EK, Lim CT, Leong KW. Collagen-based fibrous scaffold for spatial organization of encapsulated and seeded human mesenchymal stem cells. Biomaterials 2009;30(6):1133–42.
[74] Chamberlain G, Fox J, Ashton B, Middleton J. Mesenchymal stem cells: their phenotype, differentiation capacity, immunological features, and potential for homing. Stem Cells 2007;25(11):2739–49.